Contents lists available at ScienceDirect

Composites Part B

Catalytic and antibacterial activities of green-synthesized silver nanoparticles on electrospun polystyrene nanofiber membranes using tea polyphenols

Zhenyan Liu, Jiajie Yan, Yue-E Miao, Yunpeng Huang, Tianxi Liu[*]

State Key Laboratory of Molecular Engineering of Polymers, Department of Macromolecular Science, Fudan University, Shanghai 200433, PR China

ABSTRACT

An efficient and environmentally friendly method has been developed to prepare Ag nanoparticles (AgNPs) coated tea polyphenols/polystyrene (Ag-TP/PS) nanofiber membrane, which combines electrospinning and *in situ* reduction of $[Ag(NH_3)_2]^+$ using TP as the reductant and stabilizer. In this method, TP/Pluronic/PS nanofiber membranes are fabricated by electrospinning and then immersed in the aqueous solution of $[Ag(NH_3)_2]^+$. While TP is being released from TP/Pluronic/PS nanofibers, the surface of TP/Pluronic/PS nanofibers could function as reactive sites for reduction of $[Ag(NH_3)_2]^+$ without any extra reagents. XRD results indicate that AgNPs thus formed are in metallic form of Ag^0. SEM images show that AgNPs can be densely and uniformly coated on the surface of TP/Pluronic/PS nanofibers. The as-prepared Ag-TP/PS nanofiber membranes exhibit excellent catalytic properties for the degradation of methylene blue. Furthermore, the effect of $[Ag(NH_3)_2]^+$ concentration on the morphology and catalytic activity of the membrane is investigated. In addition, the antibacterial assays reveal that Ag-TP/PS nanofiber membrane possesses extraordinary antibacterial activity against both Gram-positive *Staphylococcus aureus* and Gram-negative *Escherichia coli* microorganisms. The free-standing membrane is flexible and easy to handle, which is promising for potential applications in catalysis, antibacterial agents and water remediation fields.

© 2015 Elsevier Ltd. All rights reserved.

1. Introduction

Noble metal nanoparticles have been widely used in various technological applications because of their unique optical, electronic, and catalytic properties [1–5]. Among them, Ag nanoparticles (AgNPs) have attracted much attention due to their distinctive properties, such as good conductivity, chemical stability, catalytic and antibacterial activity [6–12]. A number of efforts have been made to synthesize well-dispersed and size controllable AgNPs [2,13–16]. Chemical reduction is one of the most commonly used methods for the fabrication of AgNPs as stable and colloidal dispersions in water or organic solvents, with borohydride, hydrazine and elemental hydrogen usually used as reductants [3,17,18]. Although those are highly active, their potential to cause environmental problems seriously hinders their practical applications. Thus, an easy and environmentally friendly way to prepare

AgNPs remains a great challenge. The green synthesis of AgNPs includes selection of solvent medium, reductant and non-toxic substance (stabilizer or capping agent) for the stabilization of AgNPs [19]. There have already been many green-chemistry methods for the synthesis of AgNPs, including biological (plant extracts and microorganisms), modified Tollens, irradiation, and polyoxometalates methods [17,20,21]. Among them, utilization of plantextracts is popular owing to its wide variety of sources that are easily accessible and safe to handle. Tea polyphenols (TP) compounds, which are found naturally in tea, are flavonoids and water-soluble reductant. Previous reports showed that they could be exploited for stabilization as well as reduction of metal nanoparticles without any extra reagents or treatment [22,23]. Varma et al. revealed that spherical silver nanoparticles of controllable size distributions could be fabricated by reducing silver nitrate insolutions of tea extract or epicatechin of varying concentrations [24]. However, the spontaneous aggregation of AgNPs to minimize their surface energy will cause severe loss of specific surface area and decrease catalytic and antibacterial activities. To overcome this shortcoming, many different strategies have been developed,

* Corresponding author. Tel.: +86 21 55664197.
  E-mail address: txliu@fudan.edu.cn (T. Liu).

mainly focused on the introduction of AgNPs to high-surface-area matrices [25].

Electrospinning technique provides a versatile approach for the convenient fabrication of continuous fibers with diameters ranging from tens to hundreds of nanometers. The polymer nanofiber membranes obtained by electrospinning are flexible with high porosity and surface-area-to-volume ratio, which are ideal substances for tissue engineering scaffolds, catalytic carriers and filter materials [26,27]. They also possess the advantage of easy manipulation and retrieve over nanoparticle matrices, therefore leading to a wide variety of applications. There are generally two approaches to incorporating AgNPs in/onto nanofibers: one implies the inclusion of AgNPs in polymer during the electrospinning process, and the other relies on the deposition of AgNPs on nanofibers during the post-treatment process [28,29]. For example, Du et al. proposed a green and simple method for preparation of highly uniform and well-dispersed AgNPs (5–7 nm) embedded in electrospun PVA nanofibers by combining electrospinning technique and an *in situ* reduction approach by TP [30]. Zhang et al. showed that AgNPs-filled nylon 6 nanofibers exhibited a steady and long-lasting silver ion release behavior, and robust antibacterial activity [31]. However, immobilization of AgNPs with well-controlled shape, size, and distribution on the surface of electrospun nanofibers still poses a challenge. Therefore, surface modification of nanofibers by deposition or fabrication of AgNPs has received increasing attention, because it is desirable or necessary in certain cases [32,33]. Particularly, the method of deposition of AgNPs on nanofibers via wet-chemistry reactions has several advantages due to the capability to precisely control the size, shape, and assembly of AgNPs [34]. Furthermore, AgNPs immobilized on the surface of nanofibers can exhibit improved performance because of direct contact with the surroundings, compared with AgNPs embedded in nanofibers [35,36]. For instance, flexible and highly sensitive surface-enhanced Raman scattering (SERS) substrates were prepared by electroless plating of AgNPs on the surface of electrospun nanofibers via seed-mediated growth process [37].

Thus, hierarchical nanostructures with a number of prospective applications can be realized by combining the functionalities of AgNPs with the intrinsic properties of electrospun nanofibers, including high surface-area-to-volume ratio. In this work, we present a simple and green method to synthesize AgNPs-coated TP/polystyrene (Ag-TP/PS) nanofibers via electrospinning and *in situ* reduction using TP as the reductant and stabilizer. The membranes thus obtained have large specific surface area and an open structure. Therefore, the membranes exhibit good flexibility, high efficiency and stability as catalysts for the degradation of organic dyes, and excellent performance as antibacterial agents against *Staphylococcus aureus* (*S. aureus*) and *Escherichia coli* (*E. coli*). Moreover, the influence of $[Ag(NH_3)_2]^+$ concentration on the morphology and catalytic activity of the membranes is also investigated.

2. Experimental

2.1. Materials

Polystyrene (PS, Mw = 250,000 g/mol) was purchased from J&K Scientific Ltd. Triblock copolymer poly(ethyleneglycol)-*b*-poly(-propylene glycol)-*b*-poly(ethylene glycol) (Pluronic P123, Mn = 5800) was commercially obtained from Sigma–Aldrich. Tea polyphenols (TP) were supplied by Xuancheng Baicao Plant Industry and Trade Co., Ltd. All other reagents were purchased from Sinopharm Chemical Reagent Co., Ltd., and used without further purification.

2.2. Preparation of electrospun tea polyphenols/pluronic/ polystyrene (TP pluronic/PS) nanofiber membranes

PS and Pluronic (w/w = 7/3) were dissolved in N,N-dimethylformamide (DMF) at a concentration of 12 wt %, and a calculated amount of TP (25 wt % TP/PS-Pluronic) was added to the solution. The mixture was vigorously stirred for 10 h at room temperature to produce a clear brown solution. Then, the solution was transferred into a plastic syringe and fed at a speed of 1.0 mL/h with a distance of 15 cm between the needle tip and collector. The applied voltage was fixed at 14 kV. The fiber membrane was collected on aluminum foil and then peeled off. In addition, PS nanofiber membrane was prepared according to the literature for comparison [38].

2.3. Preparation of Ag-TP/PS nanofiber membranes

The as-prepared TP/Pluronic/PS membranes were immersed in a freshly prepared aqueous solution of $[Ag(NH_3)_2]^+$ (0.05, 0.2 and 0.5 mol/L, respectively) at room temperature for 0.5 h. After the reaction, membranes were washed with deionized water for several times and dried overnight in an oven at 40 °C. The samples were labeled as 0.05 M Ag-TP/PS, 0.2 M Ag-TP/PS and 0.5 M Ag-TP/PS, respectively. The whole preparation procedure of Ag-TP/PS nanofiber membrane is schematically shown in Fig. 1.

2.4. Characterization

X-ray diffraction (XRD) experiments were conducted on a PANalytical (X'Pert PRO) X-ray diffractometer using CuKα radiation ($\lambda = 0.1542$ nm) at an acceleration voltage of 40 kV and a current of 40 mA. Scanning electron microscopy (SEM, Tescan) performed at an acceleration voltage of 20 kV was used to observe the morphology of samples. The diameter of electrospun nanofibers and AgNPs was measured by Adobe Photoshop CS3 software from the SEM images. The surface composition of nanofibers was characterized using an energy-dispersive X-ray spectroscopy (EDX) in SEM. Static contact angles were measured using a commercial drop shape analysis system (Data Physics SCA20).

2.5. In vitro TP release

The dried TP/Pluronic/PS nanofiber membranes were cut into small square pieces (4.0 cm × 4.0 cm, 50–70 μm thick). Each specimen was exactly measured for initial weight (about 15 mg) and immersed in 25 mL of deionized water in vials. At selected time intervals, 3 mL solution was taken out and measured for TP concentrations using a Lambda-35UV–vis spectrophotometer (Perkin–Elmer) at 274 nm. These experiments were conducted in triplicate.

2.6. Measurements of the catalytic activities

Methylene blue (MB) was selected as the model dye indicator to evaluate the catalytic properties of the catalysts. The membrane of 1.0 cm × 1.0 cm (4 mg) was immersed into 10 mL of MB solution (5 mg/L) and stored in the dark for 2 h to achieve the adsorption equilibrium for MB. Then, 0.1 mL of 1 mol/L aqueous NaBH$_4$ solution was added under nitrogen atmosphere. 3 mL of the above solution was taken out from the reaction system every 10 min and immediately analyzed by UV–vis spectrophotometer. Similar procedures were conducted for the recycling ability tests. The calibration curve of MB was prepared by measuring the absorbance of different predetermined concentrations of the samples. The
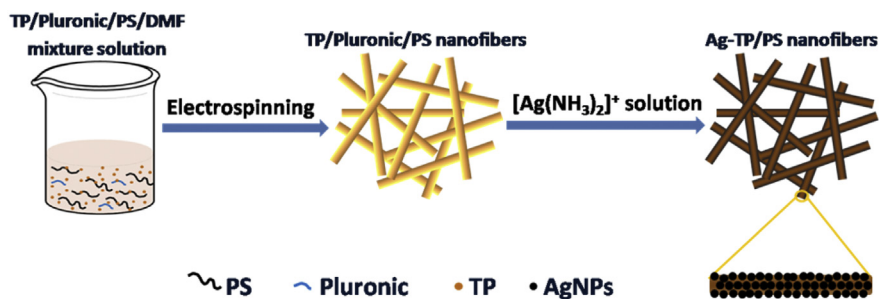
Fig. 1. Schematic illustration of the preparation of Ag-TP/PS nanofiber membrane.

catalytic activity of TP/Pluronic/PS nanofiber membrane was also carried out as the reference sample for comparison.

2.7. Antibacterial activity assays

The antibacterial activities of Ag-TP/PS nanofiber membranes were tested against both Gram-positive bacteria *S. aureus* (*S. aureus*) and Gram-negative bacteria *E. coli* (*E. coli*)by the Kirby–Bauer disk diffusion method [25,39]. From stock culture provided by School of Life Sciences at Fudan University, the microbes were inoculated in 100 mL nutrient media composed of peptone (5 g/L), NaCl (10 g/L), and beef extract (3 g/L) overnight at 37 °C with pH value maintained at 7–7.4 in the flask. Then, agar was inoculated with freshly prepared cells of each bacterium (10^7–10^8 CFU/mL) to yield a lawn of growth. After solidification of the agar, small circular pieces of PS, TP/Pluronic/PS and 0.2 M Ag-TP/PS nanofiber membranes with a diameter of 11 mm (ca. 5–8 mg) were gently placed over the agar gel in different petri dishes. After incubation at 37 °C for 24 h, the antimicrobial activity of each membrane was measured as a zone of inhibition (in mm) of the bacterial growth around the disk. The absence of an inhibition zone was interpreted as the absence of activity. These experiments were conducted in triplicate.

3. Results and discussion

3.1. Morphology and structure of Ag-TP/PS nanofiber membranes

The detailed preparation process of Ag-TP/PS nanofiber membrane is illustrated in Fig. 1. In this approach, TP/Pluronic/PS nanofibers were obtained by electrospinning and then soaked in the aqueous solution of $[Ag(NH_3)_2]^+$. While TP was gradually being released from electrospun nanofibers, $[Ag(NH_3)_2]^+$ ions were easily adsorbed onto nanofibers and reduced to AgNPs. Initially-formed AgNPs became seeds for the following nucleation and growth of AgNPs. At last, AgNPs were fully coated on the surface of nanofibers. Here, Pluronic served as the surface modifier and TP acted as both a reductant and stabilizer in this simple and green method. As the hydrophilicity of the system increases, its spinnability gets worse. To balance these two factors, the optimized Pluronic/PS weight ratio was determined through a series of experiments. Thus, the flexible TP/Pluronic/PS nanofiber membrane is shown in Fig. 2a (left). Fig. 2b shows a typical SEM image of electrospun TP/Pluronic/PS nanofibers. When compared with PS nanofibers (Fig. S1), TP/Pluronic/PS nanofibers are partially swollen. PS nanofiber membrane is hydrophobic with the water contact angle (CA) as high as 125° (Fig. S2). However, the wetting behavior of PS nanofibers has been changed into hydrophilicity by introducing Pluronic into the system (Movie S1) [40].

Supplementary video related to this article can be found at http://dx.doi.org/10.1016/j.compositesb.2015.04.037.

The incorporation of Pluronic can remarkably increase the uptake of water molecules into PS nanofibers, promoting the diffusion of TP molecules. *In vitro* TP release profile from TP/Pluronic/PS nanofibers is presented in Fig. 3. At room temperature, the release rate is fast in 1 h, and then gradually slows down. The release process reaches equilibrium 3 h later, with over 80% of the total amount of TP released. Thus, TP/Pluronic/PS nanofibers can function as reactive sites for reduction of $[Ag(NH_3)_2]^+$. The release rate is the fastest in the first 0.5 h. Therefore, it is chosen as the reaction time. As shown in Fig. 2a, the color of TP/Pluronic/PS membrane is changed from light yellow (left) to brown (right) (in the web version) after immersion in an aqueous solution of $[Ag(NH_3)_2]^+$, providing evidence for the formation of Ag nanoparticles on the nanofiber surfaces. The chemical reaction process is recorded in Movie S2. Meanwhile, the morphology and integrity of the membrane are retained well (Fig. 2b), with the mean diameter of nanofibers reduced from 615 ± 166 nm (Fig. 2b) to 569 ± 91 nm (Fig. 2c). As can be seen from Fig. 2d, the nanofibers after silver coating exhibit a relatively rough surface, in contrast to the as-electrospun nanofibers with a smooth surface. AgNPs with a diameter of 32 ± 18 nm are homogeneously covered on the surface of TP/Pluronic/PS nanofibers. The *in situ* reduction of $[Ag(NH_3)_2]^+$ on TP/Pluronic/PS nanofiber surface serving as nucleation sites or growth template can effectively prohibit the agglomeration of AgNPs. Hence, AgNPs can be densely and uniformly distributed on the surface of TP/Pluronic/PS nanofibers.

Supplementary video related to this article can be found at http://dx.doi.org/10.1016/j.compositesb.2015.04.037.

The presence of AgNPs on nanofibers was further confirmed by XRD and EDX measurements. Fig. 4 shows the XRD patterns of TP/Pluronic/PS and Ag-TP/PS membranes. Fig. 4, curve (a) exhibits a diffuse pattern indicative of the amorphous nature of PS. In the XRD pattern of Ag-TP/PS membrane (curve b), four diffraction peaks at 2θ values of 38.1°, 43.9°, 64.6° and 77.5° corresponding to (111), (200), (220) and (311) crystal planes, respectively, show the typical *fcc* structure of metallicsilver [41]. Moreover, the elemental Ag signals in the EDS spectrum (Fig. S3) demonstrate the presence of elemental Ag, indicating that AgNPs are successfully synthesized and immobilized onto TP/Pluronic/PS nanofibers by the *in situ* reduction of $[Ag(NH_3)_2]^+$ with TP. Au signal detected for EDS mapping is from the gold film sputter-coated onto the nanofiber membrane for SEM observations.

The concentration of $[Ag(NH_3)_2]^+$ has a significant influence on the morphology of Ag-TP/PS membrane (as shown in Fig. 5). When the concentration of $[Ag(NH_3)_2]^+$ is low (0.05 M) (Fig. 5a), a small amount of AgNPs with a diameter of 21 ± 13 nm is deposited on the surface of TP/Pluronic/PS nanofibers, whereas some areas of TP/Pluronic/PS nanofibers cannot be fully covered by AgNPs. Further increase in the concentration of $[Ag(NH_3)_2]^+$ can ensure the dense coating of TP/Pluronic/PS nanofibers by AgNPs (Fig. 5b). However, when the concentration of $[Ag(NH_3)_2]^+$ in the reaction system is
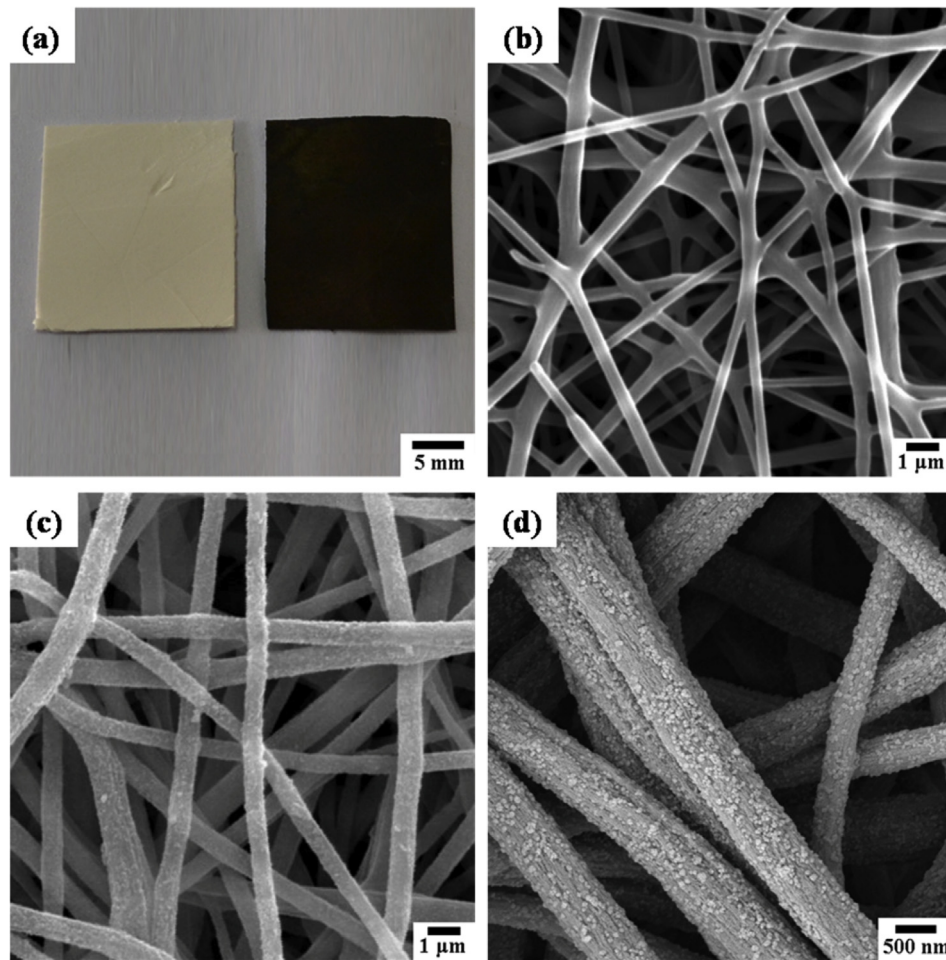
Fig. 2. (a) Digital photo of TP/pluronic/PS membrane (left) and Ag-TP/PS membrane (right); SEM images of TP/pluronic/PS membrane (b) and Ag-TP/PS membrane at low (c) and high (d) magnifications.

increased to 0.5 M (Fig. 5c), the excessive AgNPs are unevenly distributed and tend to aggregate on the surface of TP/Pluronic/PS nanofibers. In summary, these results demonstrate that the particle size and coverage degree of AgNPs on the TP/Pluronic/PS nanofibers can be easily controlled through altering the concentration of $[Ag(NH_3)_2]^+$.
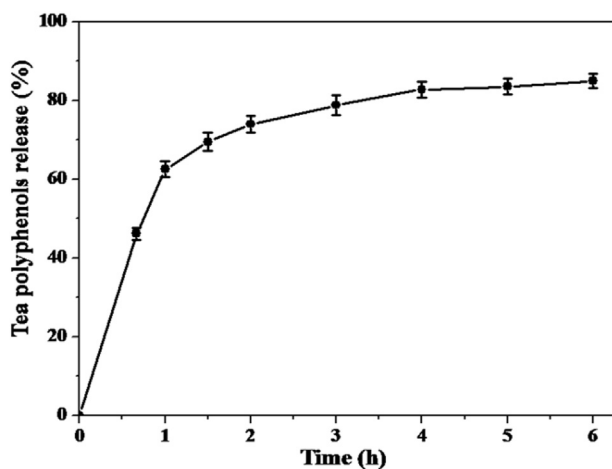
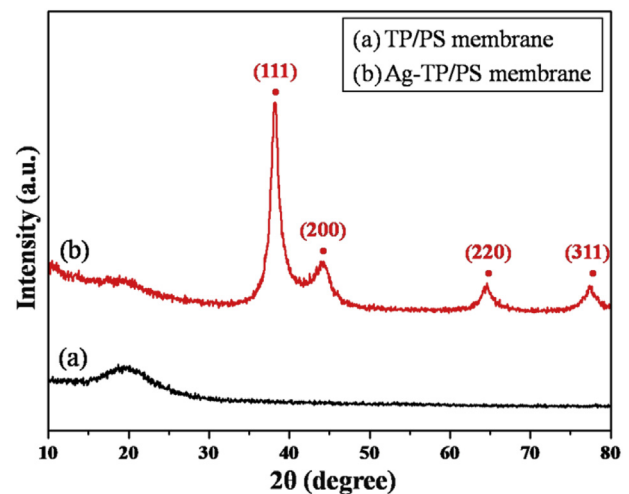**Fig. 3.** *In vitro* tea polyphenols release profile from TP/pluronic/PS membrane.

Fig. 4. XRD patterns of TP/pluronic/PS membrane and Ag-TP/PS membrane.

3.2. Catalytic activity of Ag-TP/PS nanofiber membranes

AgNPs exhibit excellent catalytic activity, which is superior to their bulk counterparts. Especially, they have been studied as catalysts in reduction reactions of nitrophenols, nitroanilines, and
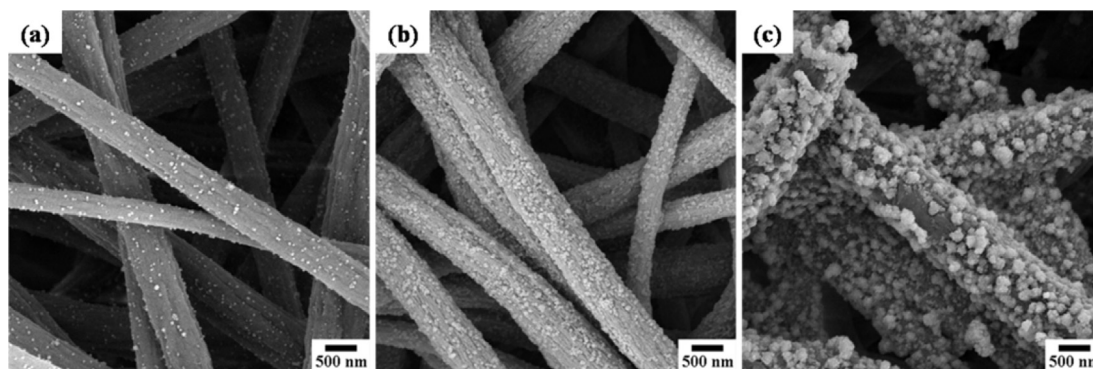
Fig. 5. SEM images of TP/pluronic/PS nanofiber membranes coated with AgNPs at different concentrations of $[Ag(NH_3)_2]^+$: (a) 0.05 M; (b) 0.2 M; and (c) 0.5 M.

various dyes [42]. To evaluate the catalytic activities of Ag-TP/PS nanofiber membranes, the degradation of MB with $NaBH_4$ as a reducing agent has been carried out. Before the catalytic degradation of MB, the catalyst was immersed in the reaction solution and kept in the dark for 2 h in each condition to ensure the adsorption–desorption equilibrium. The absorbance values of MB at 665 nm were chosen to quantitatively demonstrate the catalytic performance. Fig. 6a shows the time dependent UV–vis spectra of the MB solution in the presence of 0.2 M Ag-TP/PS. The absorbance at λ_{max} of MB is obviously decreased with time, indicating an efficient degradation of MB on the membrane. The whole degradation process can be visually depicted in the digital photos, as shown in the insets of Fig. 6a. To describe the effect of catalytic degradation, we define:

$$Degradation\ (\%) = (C_0 - C)/C_0 \times 100$$

where C_0 is the initial concentration of MB, C is the concentration of MB at time t. As is evident from Fig. 6b, the absence of any catalysts (but in the presence of $NaBH_4$) in MB solution only results in a slight degradation after 60 min. The degradation of MB in the presence of Ag-TP/PS membrane (without $NaBH_4$) is negligible. The TP/Pluronic/PS nanofiber membrane has no notable effect on degradation of MB, while MB is obviously degraded with Ag-TP/PS membrane. The MB solution is degraded by 93% in 60 min with the 0.2 M Ag-TP/PS membrane, which is higher than those with the 0.05 M and 0.5 M Ag-TP/PS membranes. The above results reveal that the concentration of $[Ag(NH_3)_2]^+$ significantly influences the catalytic activity of the as-prepared catalysts.

The three-dimensional porous structure of Ag-TP/PS nanofiber membrane provides large contact area between the catalyst and water solution, greatly promoting diffusion of MB and the catalytic degradation reaction. Thus, TP/Pluronic/PS nanofiber membrane covered with uniform and dense AgNPs proves to be an effective catalyst. Moreover, the concentration of $[Ag(NH_3)_2]^+$ has a significant effect on the degradation of MB as well as the morphology of Ag-TP/PS membrane. The catalytic activity of Ag-TP/PS membrane initially increases and then decreases with the increase in concentration of $[Ag(NH_3)_2]^+$. The optimum concentration of $[Ag(NH_3)_2]^+$ is 0.2 M, where there is a trade-off between coverage degree and specific surface area. On one hand, reactive surface area increases with the increase in AgNPs coverage. On the other hand, high amount of AgNPs loading makes the size of AgNPs increase, resulting in a dramatic decrease of specific surface area [25,36]. When the concentration of $[Ag(NH_3)_2]^+$ surpasses the threshold value, the aggregation of AgNPs extensively occurs. Consequently, the number of catalytic active sites decreases and the degradation
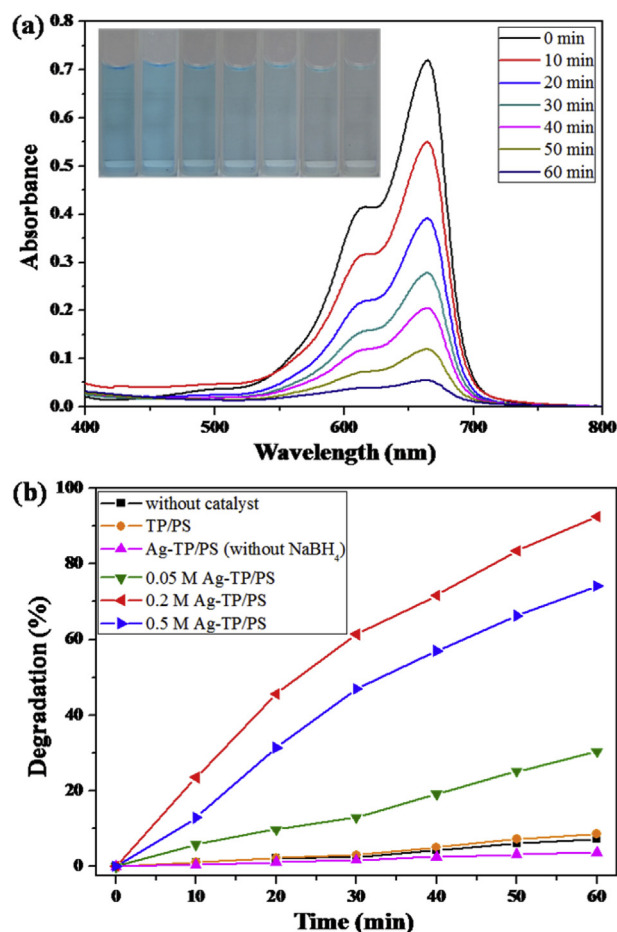

Fig. 6. Time dependent UV–vis absorption spectra of MB solution with 0.2 M Ag-TP/PS membrane for the first cycle (a), and catalytic degradation curves of MB on Ag-TP/PS nanofiber membranes with different concentrations of $[Ag(NH_3)_2]^+$ (b). The insets in (a) are the corresponding digital photos of MB solutions at the same time when the UV–vis spectra are taken.

of the dye pollutant is affected. Therefore, the concentration of $[Ag(NH_3)_2]^+$ should be adequately controlled.

Besides the catalytic efficiency, in view of practical applications, the stability and recyclability are also indispensable to catalysts. With excellent flexibility, the self-standing Ag-TP/PS nanofiber membranes could be easily taken out of solutions after use. We further studied the stability of the 0.2 M Ag-TP/PS nanofiber membrane with the best catalytic activity studied here. Fig. 7a

shows the recycling test results for the 0.2 M Ag-TP/PS membrane. The degradation of MB slightly declines from 93% to 87% after five cycles, still providing a good performance. Fig. 7b is the SEM image of the membrane after five cycles of catalytic tests. It can be seen that AgNPs are still densely immobilized on the surface of TP/Pluronic/PS nanofibers after immersion in water for about 8 h, and there is no apparent change compared with Fig. 2d. Obviously, Ag-TP/PS nanofiber membranes exhibit good catalytic stability for the degradation of dye pollutant. The 0.2 M Ag-TP/PS nanofiber membrane shows high catalytic activity, which results from two aspects. Firstly, they possess large specific surface area, providing numerous reactive sites of AgNPs; secondly, they also maintain good stability, effectively avoiding secondary pollution.

3.3. Antibacterial activity of Ag-TP/PS nanofiber membrane

Ag is extensively used as an effective antimicrobial agent against different bacteria [43], virus, and fungi [44]. Nevertheless, AgNPs have the potential to cause cytotoxicity and genotoxicity [45,46]. The antibacterial activity of Ag-TP/PS nanofiber membranes was investigated by using the disk-diffusion method. PS, TP/Pluronic/PS and 0.2 M Ag-TP/PS membranes were placed on agarplates, which were seeded with *S. aureus* and *E. coli*, respectively. As shown in Fig. 8, no antibacterial effects are observed for neat PS membrane. TP/Pluronic/PS membrane possesses good antibacterial activity against *S. aureus* (zone of inhibition is 20.67 ± 0.47 mm), but almost
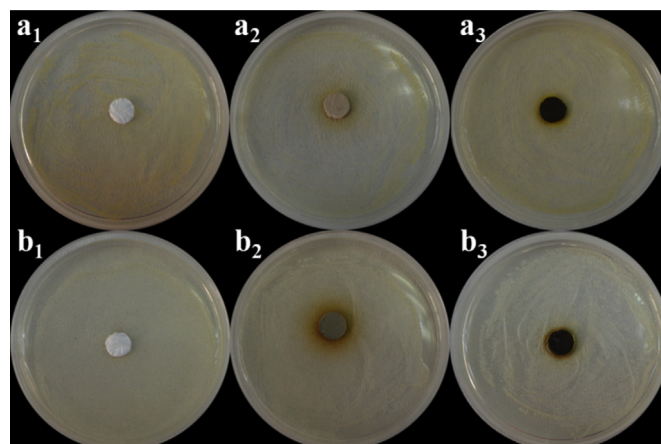

Fig. 8. Zone of inhibition tests for PS (a_1, b_1); TP/Pluronic/PS (a_2, b_2); and 0.2 M Ag-TP/PS (a_3, b_3) nanofiber membranes against *S. aureus* (a_1–a_3) and *E. coli* (b_1–b_3).

Table 1
Mean zones of inhibition for PS, TP/Pluronic/PS and 0.2 M Ag-TP/PS nanofiber membranes against *S. aureus* and *E. coli* microorganisms.

Sample	Zone of inhibition (mm)[a]	
	S. aureus	*E. coli*
PS	−	−
TP/Pluronic/PS	20.67 ± 0.47	−
0.2 M Ag-TP/PS	16.67 ± 0.47	15.30 ± 1.24

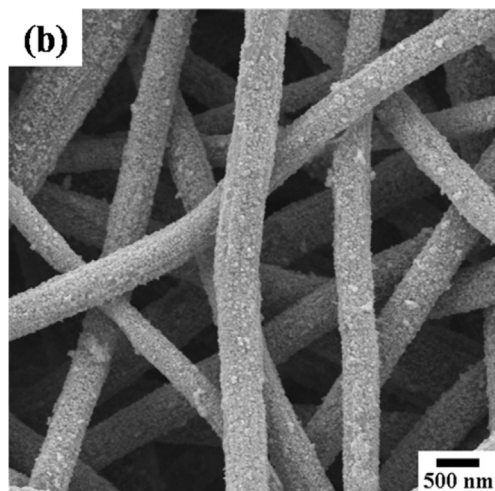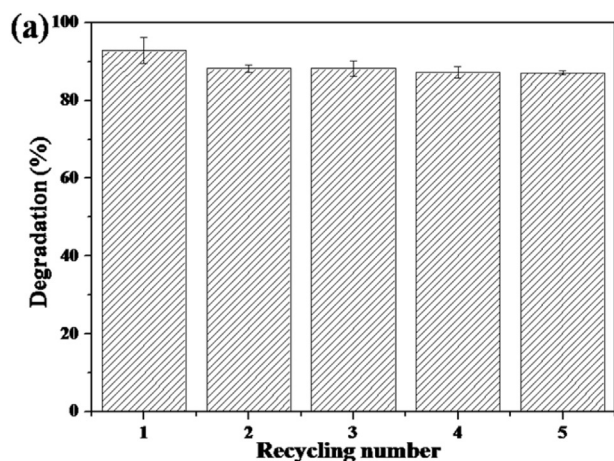[a] Average zone of inhibition diameter is based on triplicate plates.

Fig. 7. Recycling catalytic tests on 0.2 M Ag-TP/PS nanofiber membranes (a); and SEM image of the membrane after five cycles (b).

has no effect on *E. coli*, which is consistent with previous findings [47]. Toda et al. reported that TP inhibited pathogens such as *S. aureus*, *Staphylococcus epidermis*, *Plesiomonasshigelloides*, but was not effective against *E. coli*, *Pseudomonas aeruginosa* or *Aeromonashydrophila* [47]. The observation that TP is bactericidal to Gram-positive but not to Gram-negative bacteria can be explained to some extent by the presence of negatively charged lipopolysaccharide in Gram-negative bacteria [48]. The zone of inhibition around the 0.2 M Ag-TP/PS membrane is measured to be 16.67 ± 0.47 mm against *S. aureus* and15.30 ± 1.24 mm against *E. coli*. Ag-TP/PS membrane shows a smaller zone of inhibition than TP/Pluronic/PS membrane, because the content of TP is decreased after TP/Pluronic/PS membrane is immersed in the $[Ag(NH_3)_2]^+$ solution. In addition, the combination of AgNPs and TP/Pluronic/PS nanofibers exhibits slightly stronger inhibitory activity against *S. aureus* than against *E. coli*. The detailed zone of inhibition data for these samples against *S. aureus* and *E. coli* are also listed in Table 1. These results reveal that Ag-TP/PS membranes are able to effectively inhibit bacterial growth.

4. Conclusions

In summary, we described a simple and green method to synthesize Ag-TP/PS nanofiber membranes by combining an electrospinning technique and *in situ* reduction approach. Besides the electrospinning solution, this method does not need extra reducing/stabilizing agents, or irradiation/thermal treatment. The *in situ* generation of AgNPs and the stabilization of TP result in uniform and dense coverage of AgNPs on TP/Pluronic/PS nanofibers. The composite membranes exhibit outstanding catalytic activity for the degradation of dye pollutant. The optimum concentration of $[Ag(NH_3)_2]^+$ proves to be 0.2 M, which can be attributed to the balance between AgNPs coverage and specific

surface area. Moreover, Ag-TP/PS nanofiber membranes have a good recyclable catalytic performance for the degradation of MB. And the antibacterial assays reveal that Ag-TP/PS nanofiber membranes have excellent antibacterial effect against both *S. aureus* and *E. coli*. Therefore, the flexible Ag-TP/PS composite membranes can potentially be used as recyclable catalysts for reducing the dye pollutant in the water remediation and as antibacterial agents for medical and environmental applications.

Acknowledgment

Appendix A. Supplementary data

Supplementary data related to this article can be found at http://dx.doi.org/10.1016/j.compositesb.2015.04.037.

References

[1] Liu AP, Dong WJ, Liu EJ, Tang WH, Zhu JQ, Han JC. Electrochim Acta 2010;55: 1971—7.
[2] Ko S, Banerjee CK, Sankar J. Compos Part B Eng 2011;42:579—83.
[3] Zhang SZ, Ni WH, Kou XS, Yeung MH, Sun LD, Wang JF, et al. Adv Funct Mater 2007;17:3258—66.
[4] Lei Y, Mehmood F, Lee S, Greeley J, Lee B, Seifert S, et al. Science 2010;328: 224—8.
[5] Liu FJ, Yuan Y, Li L, Shang SM, Yu XH, Zhang Q, et al. Compos Part B Eng 2015;69:232—6.
[6] Liu AP, Zhu JQ, Han JC, Wu HP, Jiang CZ. Electrochem Commun 2008;10: 827—30.
[7] Zhang P, Shao CL, Zhang ZY, Zhang MY, Mu JB, Guo ZC, et al. Nanoscale 2011;3: 3357—63.
[8] Mizuuchi K, Inoue K, Agari Y, Sugioka M, Tanaka M, Takeuchi T, et al. Compos Part B Eng 2012;43:1445—52.
[9] Wang RY, Guo J, Chen D, Miao YE, Pan JS, Tjiu WW, et al. J Mater Chem 2011;21:19375—80.
[10] Liu XN, Xue G, Lu Y, Zhang J, Li FT, Xue CC, et al. Chin J Polym Sci 2001;19: 265—8.
[11] Koo Y, Littlejohn G, Collins B, Yun YH, Shanov VN, Schulz M, et al. Compos Part B Eng 2014;57:105—11.
[12] Chen X, Zheng ZF, Ke XB, Jaatinen E, Xie TF, Wang DJ, et al. Green Chem 2010;12:414—9.
[13] Li ZY, Huang HM, Shang TC, Yang F, Zheng W, Wang C, et al. Nanotechnology 2006;17:917—20.
[14] Li GY, Zhang T, Liu JW, Qi MY. Acta Polym Sin 2013:355—60.
[15] Khan A, Asiri AM, Rub MA, Azum N, Khan AAP, Khan SB, et al. Compos Part B Eng 2013;45:1486—92.
[16] Gashti MP, Almasian A. Compos Part B Eng 2012;43:3374—83.
[17] Sharma VK, Yngard RA, Lin Y. Adv Colloid Interf 2009;145:83—96.
[18] Wu ZC, Zhang Y, Tao TX, Zhang LF, Fong H. Appl Surf Sci 2010;257:1092—7.
[19] Roy N, Gaur A, Jain A, Bhattacharya S, Rani V. Environ Toxicol Pharmacol 2013;36:807—12.
[20] Nadagouda MN, Speth TF, Varma RS. Acc Chem Res 2011;44:469—78.
[21] Cao XW, Ding B, Yu JY, Al-Deyab SS. Carbohydr Polym 2013;92:571—6.
[22] Shao SJ, Li L, Yang G, Li JR, Luo C, Gong T, et al. Int J Pharm 2011;421:310—20.
[23] Fei YN, Chen Y, Wang HB, Gao WD, Yang RH, Wan YQ. Fibers Polym 2011;12: 340—4.
[24] Moulton MC, Braydich-Stolle LK, Nadagouda MN, Kunzelman S, Hussain SM, Varma RS. Nanoscale 2010;2:763—70.
[25] Deng ZW, Zhu HB, Peng B, Chen H, Sun YF, Gang XD, et al. ACS Appl Mater Interfaces 2012;4:5625—32.
[26] Cipitria A, Skelton A, Dargaville TR, Dalton PD, Hutmacher DW. J Mater Chem 2011;21:9419—53.
[27] Wang XF, Ding B, Sun G, Wang MR, Yu JY. Prog Mater Sci 2013;58:1173—243.
[28] Radetic M. J Mater Sci 2013;48:95—107.
[29] Zou ML, Du ML, Zhu H, Xu CS, Li N, Fu YQ. Polym Eng Sci 2013;53:1099—108.
[30] Zhu H, Du ML, Zhang M, Wang P, Bao SY, Fu YQ, et al. Sens Actuat B Chem 2013;185:608—19.
[31] Shi Q, Vitchuli N, Nowak J, Noar J, Caldwell JM, Breidt F, et al. J Mater Chem 2011;21:10330—5.
[32] Lu XF, Wang C, Wei Y. Small 2009;5:2349—70.
[33] Agarwal S, Wendorff JH, Greiner A. Macromol Rapid Commun 2010;31: 1317—31.
[34] Carlberg B, Ye LL, Liu JH. Small 2011;7:3057—66.
[35] Yu LN, Wang M, Shen LD, Wang XF, Zhu MF. Acta Polym Sin 2014:239—47.
[36] Xiao SL, Xu WL, Ma H, Fang X. RSC Adv 2012;2:319—27.
[37] Zhang LF, Gong X, Bao Y, Zhao Y, Xu M, Jiang CY, et al. Langmuir 2012;28: 14433—40.
[38] Uyar T, Besenbacher F. Polymer 2008;49:5336—43.
[39] Zheng FY, Wang SG, Wen SH, Shen MW, Zhu MF, Shi XY. Biomaterials 2013;34:1402—12.
[40] Miao YE, Zhu H, Chen D, Wang RY, Tjiu WW, Liu TX. Mater Chem Phys 2012;134:623—30.
[41] Barakat NAM, Woo KD, Kanjwal MA, Choi KE, Khil MS, Kim HY. Langmuir 2008;24:11982—7.
[42] Kang HG, Zhu YH, Yang XL, Jing YJ, Lengalova A, Li CZ. J Colloid Interf Sci 2010;341:303—10.
[43] Feng QL, Wu J, Chen GQ, Cui FZ, Kim TN, Kim JO. J Biomed Mater Res 2000;52: 662—8.
[44] Panyala NR, Pena-Mendez EM, Havel J. J Appl Biomed 2008;6:117—29.
[45] AshaRani PV, Mun G, Hande MP, Valiyaveettil S. ACS Nano 2009;3:279—90.
[46] Poornima D, Ishita M, Uday Kumar S, Abhay S, Bharat B, Gopinath P. Adv Colloid Interf 2015. http://dx.doi.org/10.1016/j.cis.2015.02.007.
[47] Toda M, Okubo S, Hiyoshi R, Shimamura T. Lett Appl Microbiol 1989;8:123—5.
[48] Ikigal H, Nakae T, Hara Y, Shimamura T. Biochim Biophys Acta 1993;1147: 132—6.